

Chapter 2

The n -modal map

Our motivation for studying multi-modal 1-dimensional maps is both because these maps are interesting chaotic systems and because as it will be shown below (chapter 4), the multi-modal maps are the approximations for the general 2-dimensional folding maps. The “finger print” of a n -modal map is the *swallowtail* bifurcation structure in the parameter space and to describe the organization of the swallowtails is one main result in this chapter. The swallowtails are also typical structures in the 2-dimensional folding maps and the methods used in this chapter will be applied for folding maps in chapter 4. We will also study here how a change of modality implies that the symbolic description may change for an unstable orbit followed adiabatically in the parameter space. This will also be the situation for the folding maps and is the main difficulty in the definition of symbolic dynamics as discussed in section 5.2.

A one dimensional continuous map $x_{t+1} = f(x_t)$ with n maximum and minimum points is called the n -modal map. This is a natural generalization of the study of unimodal maps with bifurcations and kneading sequences as the unimodal maps but with larger alphabets and more complicated bifurcations. Bifurcation diagrams for n -modal maps with $n > 2$ have not been systematically studied earlier. In chapter 4 we show that a restricted n -modal map gives the approximate description of the Hénon map, and we conjecture that such approximations are applicable to most folding flows in three dimensions.

The complete unimodal repellor, figure 1.10, has at l -th level 2^l intervals remaining in the interval $[0, 1]$. In a complete n -modal repellor a Cantor set with $(n + 1)^l$ intervals remaining at each level l , so a $(n + 1)$ -ary alphabet labels uniquely the points in the Cantor set. For example figure 2.1 shows the bimodal function

$$f(x) = x^3 - ax + b \tag{2.1}$$

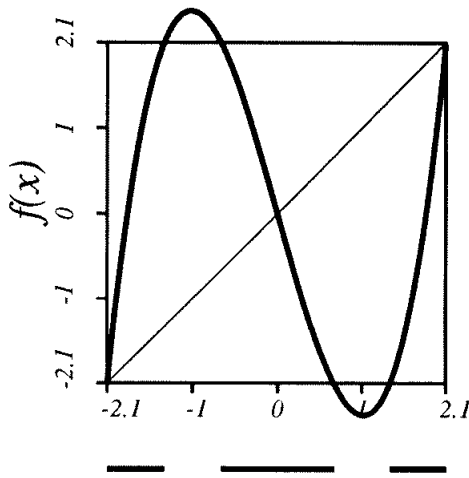


Figure 2.1: The bimodal map (2.1) with $a = 3.5$ and $b = 0$, and the intervals which have not escaped after 1 iteration.

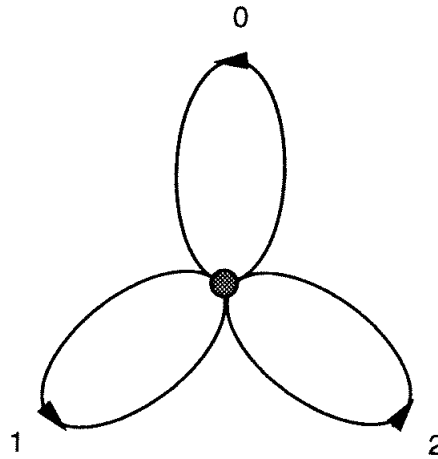


Figure 2.2: The automaton for the complete 3-ary Cantor set repeller; all symbol strings are legal.

with maximum at $x_{c1} = -\sqrt{a/3}$, and minimum at $x_{c2} = \sqrt{a/3}$, for parameter values $a = 3.5$ and $b = 0$. The 3 intervals are labeled by the alphabet $s \in \{0, 1, 2\}$ and the automaton graph in figure 2.2 generates all admissible strings of the three symbols.

One example of a trimodal map is given by the function

$$f(x) = cx^4 + x^3 - ax + b \quad (2.2)$$

drawn in figure 2.3 for $a = 5.85$, $b = 2.8$ and $c = 0.15$. The repeller is here a complete 4-interval Cantor set.

We shall enumerate the n -modal map critical points; $x_{c1}, x_{c2}, \dots, x_{cn}$ from left to right. The symbol corresponding to a point x_t is

$$s_t = \begin{cases} 0 & \text{if } x_t < x_{c1} \\ i & \text{if } x_{ci} < x_t < x_{c(i+1)} \\ n & \text{if } x_t > x_{cn} \end{cases} \quad (2.3)$$

For convenience we choose $f'(x) > 0$ for $x_t < x_{c1}$. In that case $f'(x) > 0$ for s_t even and $f'(x) < 0$ for s_t odd, and x_{ci} is a maximum if i is odd and a minimum if i is even. Choosing $f'(x) < 0$ for $x_t < x_{c1}$ gives a map with slightly different bifurcation structure which can be studied by the same method. As for the unimodal map, the ordering of symbols has to be reversed when $f'(x) < 0$, *i.e.* for s_t odd. The well ordered symbolic value of the point x_0 with future symbol string $s_1 s_2 s_3 \dots$ is

$$\tau = 0.w_1 w_2 w_3 \dots = \sum_{t=1}^{\infty} \frac{w_t}{(n+1)^t} \quad (2.4)$$

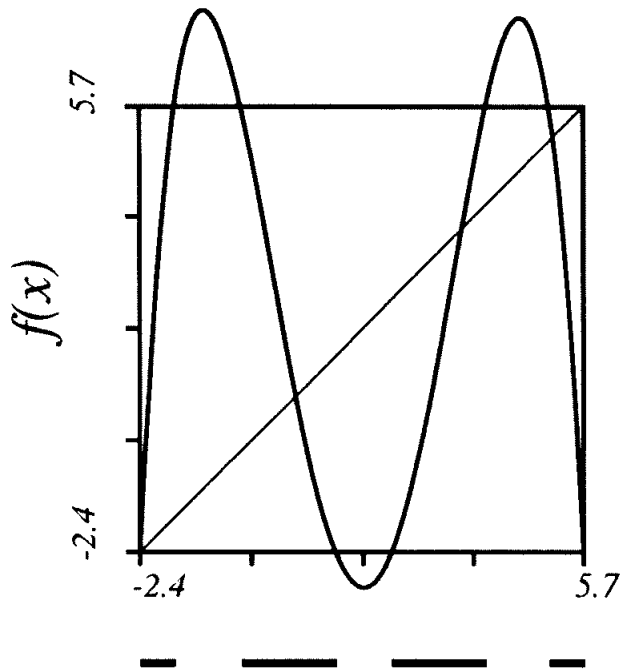


Figure 2.3: The 3-modal map (2.1 with $a = 5.85$, $b = 2.8$ and $c = 0.15$ and the remaining intervals after 1 iteration.

where w_t is given recursively by

$$\begin{aligned} w_1 &= s_1 \\ p_1 &= \begin{cases} 1 & \text{if } s_1 \text{ even} \\ -1 & \text{if } s_1 \text{ odd} \end{cases} \\ \\ w_t &= \begin{cases} s_t & \text{if } p_{t-1} = 1 \\ (n - s_t) & \text{if } p_{t-1} = -1 \end{cases} \\ p_t &= \begin{cases} p_{t-1} & \text{if } s_t \text{ even} \\ -p_{t-1} & \text{if } s_t \text{ odd} \end{cases} \end{aligned} \tag{2.5}$$

In the unimodal case is $n = 1$ and the algorithm (2.4) reduces to algorithm (1.18). If $f'(x) < 0$ for $x_t < x_{c1}$ we have the same algorithm but with the inverted values of p_t .

The n critical points $x_{c1}x_{c2} \dots x_{cn}$ yield n different kneading sequences $K_1K_2 \dots K_n$, and n kneading values $\kappa_1\kappa_2 \dots \kappa_n$. As for the unimodal map, the critical points bound the extreme x values an orbit can have. The i -th critical point x_{ci} restricts the value $f(x)$ can take on the interval $x_{c(i-1)} < x < x_{c(i+1)}$. For a point x between two critical points, the value $f(x)$ is smaller than the closest maximum point and larger than the closest minimum point.

The admissibility (pruning) condition for orbit S is

$$\begin{aligned} \tau_i^{\max}(S) &\leq \kappa_i & \text{for } i \text{ odd} \\ \tau_i^{\min}(S) &\geq \kappa_i & \text{for } i \text{ even} \end{aligned} \tag{2.6}$$

The index i on τ restricts x_0 to the appropriate interval, $s_0 = i - 1$ or $s_0 = i$. If $s_0 = 0$ there is no explicit minimum restriction, and if $s_0 = n$ there is no explicit maximum (minimum) restriction if n is even (odd).

One complication is that as the parameters vary a map may lose some of the critical points. A maximum and a minimum point x_{ci} and $x_{c(i+1)}$ may merge, reducing the function $f(x)$ to have $(n - 2)$ critical points and making the map $(n - 2)$ -modal. The symbol $s \in \{i - 1, i, i + 1\}$ are then indistinguishable and a symbol $i - 1$ can be changed to $i + 1$ by smoothly changing parameters. This bifurcation is important because it implies that orbits change symbolic description without becoming stable and this bifurcation is unavoidable in the description of two-dimensional maps. We will return to this in section 2.2 and in section 5.2.1.

2.1 Bimodal maps

The simplest example of a multimodal map is the bimodal map. The bifurcation structure of real bimodal maps has been investigated by MacKay, Tresser, van

Zeijts, Glass, Milnor, Fraser, Kapral and others [19, 78, 79, 86, 140, 141, 142, 151]. The complex bimodal map has also been studied by Branner, Douady, Hubbard and Milnor [30, 63, 150]. Scaling relations for bifurcations in these maps are obtained by MacKay and van Zeijts [142]. The bimodal bifurcation is a typical bifurcation inside an Arnold tongue and a general phenomena observable in most dissipative dynamical systems. In figures 2.4, 2.6 and 2.8 we show the parameter regions where some short orbits of the map (2.1) are stable and these are the typical bimodal swallowtails.

If we scan the parameter space of a bimodal map by varying only one parameter then we would find a sequence of bifurcations and inverse bifurcations which would be hard to make any sense of, while in a two dimension parameter space the bifurcation structures can be explained. A good way to represent bimodal maps is to use the kneading values as the topological parameters or symbolic parameters (see discussion below). In the topological parameter space (κ_1, κ_2) the bifurcations have a universal form common to all bimodal maps, in the same sense that the MSS ordering in the unimodal κ parameter is universal.

From 2.6 it follows that an orbit S is admissible in the bimodal map if

$$\tau^{\max}(S) < \kappa_1 \quad (2.7)$$

$$\tau^{\min}(S) > \kappa_2 \quad (2.8)$$

The area of the (κ_1, κ_2) parameter plane for which a given orbit S exists is given by the inequalities (2.7) and (2.8).

The shortest periodic orbits $\bar{1}$, $\overline{21}$, $\overline{20}$ and $\overline{10}$ exist for the kneading values

$$\begin{aligned} \bar{1} & \text{ exists if } \kappa_1 \geq 0.\bar{1} = 1/2 & \text{ and } \kappa_2 \leq 0.\bar{1} = 1/2 \\ \overline{21} & \text{ exists if } \kappa_1 \geq 0.\overline{2101} = 4/5 & \text{ and } \kappa_2 \leq 0.\overline{1012} = 2/5 \\ \overline{20} & \text{ exists if } \kappa_1 \geq 0.\overline{20} = 3/4 & \text{ and } \kappa_2 \leq 0.\overline{02} = 1/4 \\ \overline{10} & \text{ exists if } \kappa_1 \geq 0.\overline{1210} = 3/5 & \text{ and } \kappa_2 \leq 0.\overline{0121} = 1/5 \end{aligned} \quad (2.9)$$

The regions in the topological parameter plane for which the periodic orbits $\bar{1}$, $\overline{21}$, $\overline{20}$ and $\overline{10}$ exist are the rectangles drawn in figure 2.5.

This pattern, which we call a swallow tail, should be compared with the stable period 2 orbit in the parameter plane (a, b) in figure 2.4. The diagonal $\kappa_2 = 1 - \kappa_1$ is a symmetry axis and corresponds to $b = 0$ in eq. (2.1).

The area in (κ_1, κ_2) for which the symbol string $\bar{1}$ is admissible corresponds to the values of κ_1 and κ_2 for which there exists a fixed point between x_{c1} and x_{c2} . But in addition, the symbol string $\bar{1}$ describes the stable period 2 orbit that bifurcates from the fixed point before it reaches the super stable value. This period 2 orbit may become super-stable if the left point in the orbit reaches the critical

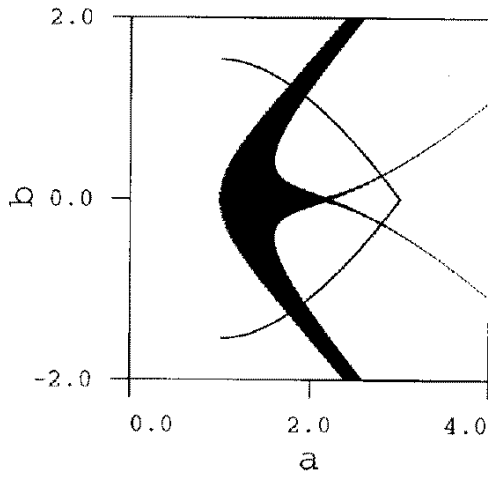


Figure 2.4: The area in parameter plane (a, b) of the bimodal map (2.1) where period 2 orbits are stable together with the curves corresponding to the “one Ulam” map.

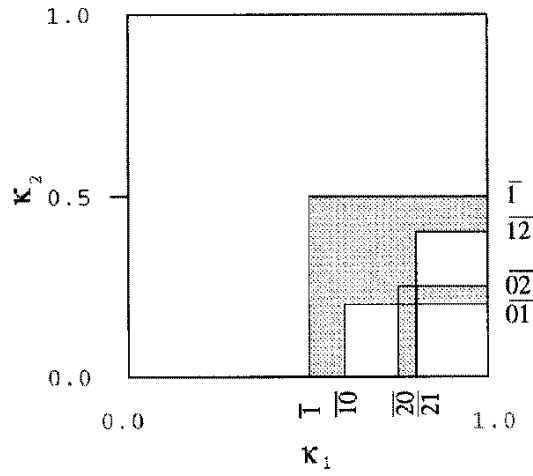


Figure 2.5: The areas in the topological parameter space of the bimodal map where the periodic orbits $\overline{1}$, $\overline{21}$, $\overline{20}$ and $\overline{10}$ exist.

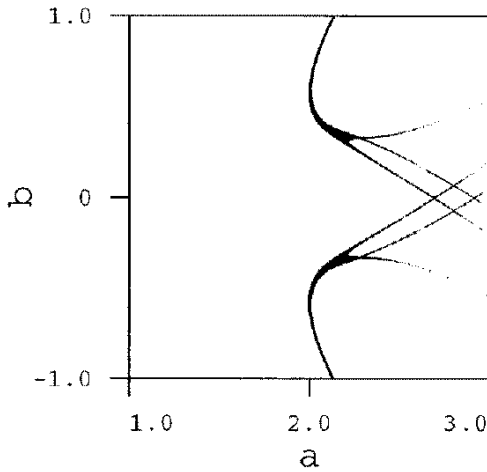


Figure 2.6: The area in the parameter plane (a, b) of the bimodal map (2.1) for which the period 3 orbits are stable.

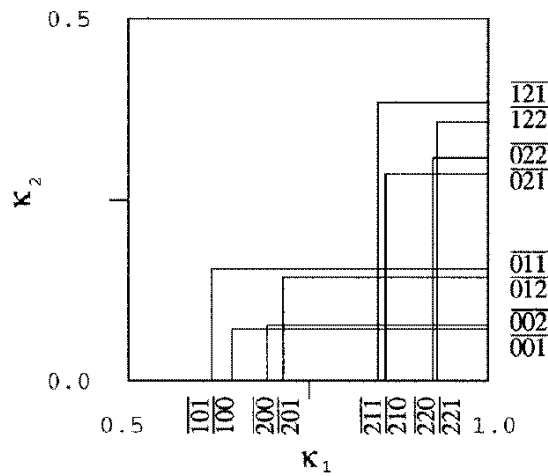


Figure 2.7: The areas in the topological parameter space of the bimodal map for which the period 3 orbits exist.

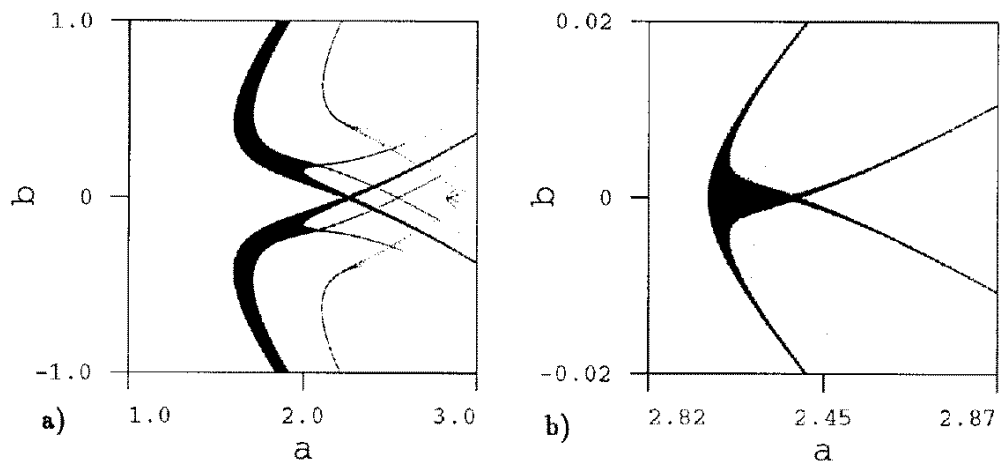


Figure 2.8: a) The area in the parameter plane (a, b) of the bimodal map (2.1) where period 4 orbits are stable. b) A magnification showing the smallest period 4 swallow tail.

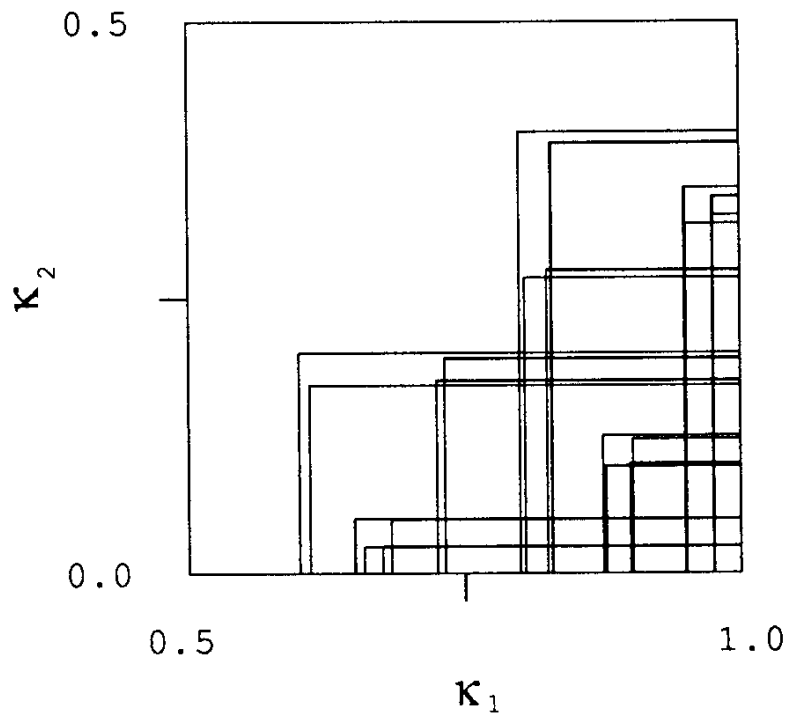


Figure 2.9: The areas in the topological parameter space of the bimodal map where the period 4 orbits exist.

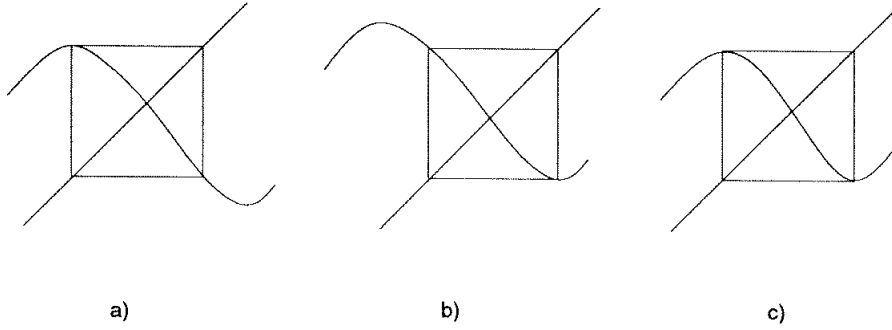


Figure 2.10: The possible super-stable period 2 orbits when the symbolic description of the orbit changes from $\bar{1}$ to a) $\bar{10}$ b) $\bar{21}$ c) $\bar{20}$.

point x_{c1} changing the symbols of the orbit to $\bar{10}$ as in figure 2.10 a), or if the right point in the orbit reaches x_{c2} changing the symbols to $\bar{21}$ as in figure 2.10 b), or if both points in the orbit reach the two critical points simultaneously changing the symbol string to $\bar{20}$ as drawn in figure 2.10 c). Up to 3 different stable orbits may be described with the symbol string $\bar{20}$. In figure 2.11 the curves in the parameter space where the orbits are super-stable are drawn as dashed curves and these curves will correspond topologically to the bifurcation lines in figure 2.5.

The figures 2.5, 2.7 and 2.9 may be interpreted in the following way. A kneading value κ jumps from κ_a to κ_b when the attracting stable orbit passes through a super stable point as showed in the unimodal map in figure 1.12. Values in the open interval $\langle \kappa_a, \kappa_b \rangle$ do not correspond to any kneading sequence, so this interval is “forbidden”. In a smooth map we can identify this empty interval with the parameter interval where a period n orbit goes from the super-stable point through a period doubling bifurcation to the super-stable period $2n$ orbit. The period doubling corresponds to one point in this interval. The areas in parameter space where the period $2n$ orbit is stable have the same topological structure as the forbidden interval areas. In figure 2.5 the forbidden areas are colored gray and we identify this area with the black area in figure 2.4; the *swallowtail*. This topological identification between structures in the real parameter space (a, b) and the kneading value space (κ_1, κ_2) motivates us to call the space (κ_1, κ_2) the *topological parameter space*. Since the values κ are a representation of the symbolic dynamics we will also use the term *symbolic parameter space*.

If one of the critical points iterates into the fixed point $\bar{0}$ all bifurcations take place at the other critical point. The lines of parameter values (a, b) where this hap-

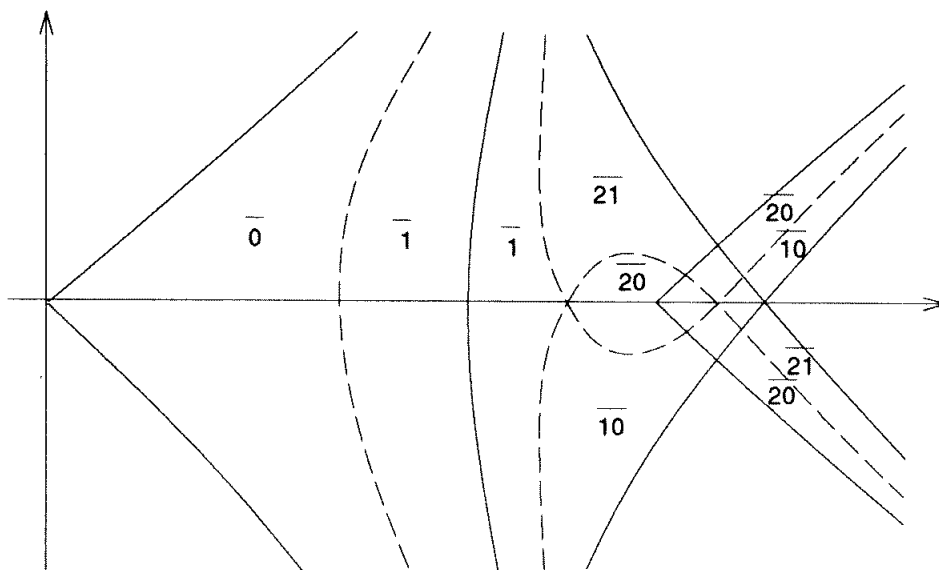


Figure 2.11: A sketch of the curves in parameter space giving bifurcations (solid curve) and super stable period 1 and period 2 orbits (dashed curve) in the bimodal map. The symbol strings for various orbits are indicated.

pens are drawn in figure 2.4; we call this a “one-Ulam” map case. For parameter values outside these Ulam curves at least one critical point iterates to infinity, and there is no swallowtail crossings, only non-crossing tails (codimension one bifurcations). The one-Ulam curves and all parameter values beyond these curves map in the topological parameter space into the two borders $\kappa_1 = 1$ and $\kappa_2 = 0$.

2.1.1 Markov graphs

The construction of the automaton graph of the bimodal map is similar to the unimodal case: the kneading sequences are drawn on a tree, forbidden branches are crossed out, and the admissible branches are reconnected into a closed graph. The bimodal case tree is more complicated than for the unimodal case tree, but there are no new important conceptual features brought in by the generalization to bimodal maps.

We work out one example, the case of two coexisting stable periodic orbits, with the repeller described by a Markov partition and a finite automaton graph. Assume that the orbits $\overline{21}$ and $\overline{100}$ are stable. From figures 2.5 and 2.7 we see that at the point $(\kappa_1, \kappa_2) = (0.\overline{2101}, 0.\overline{001221})$ the vertical line for $\overline{21}$ crosses the horizontal line for $\overline{001}$. This implies that there exists a parameter space (a, b) region for which

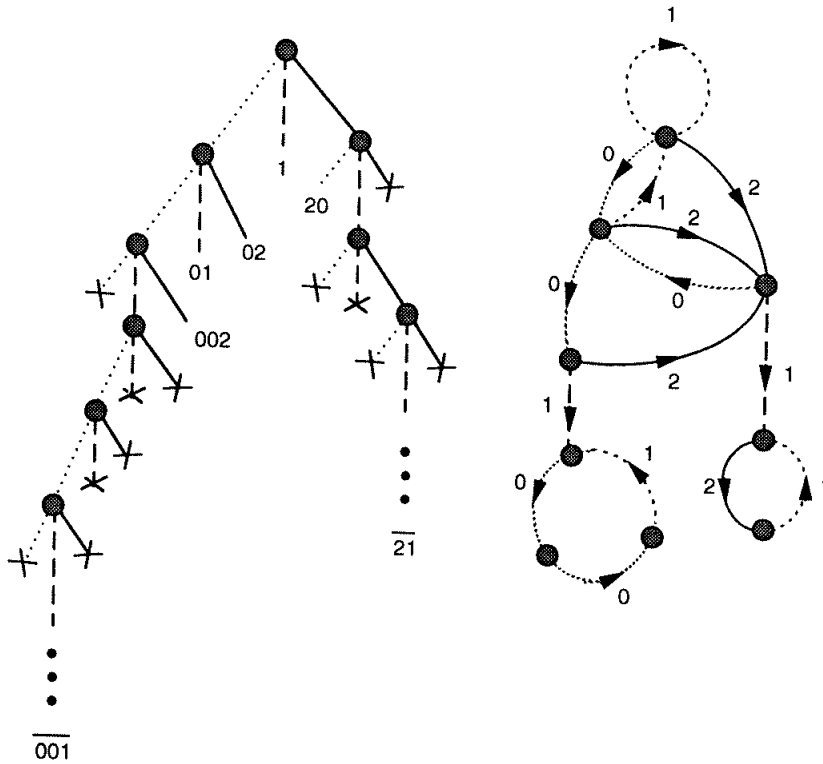


Figure 2.12: The construction of the automaton graph for the bimodal map with coexisting stable orbits $\overline{21}$ and $\overline{100}$.

both orbits are stable. Comparing figure 2.4 and figure 2.6 we see that the two tails where these orbits are stable indeed cross. Figure 2.12 shows the construction of the corresponding pruned tree and the automaton. The construction yields a transient repeller and the two attracting cycles. It misses the two loops $\overline{0}$ and $\overline{2}$ which is the two isolated unstable fixed points, and which can be drawn in the automaton as isolated transients before the transient repeller in figure 2.12. These loops will not contribute to calculations of average values like entropy (see below). Removing the two attracting cycles $\overline{100}$ and $\overline{21}$ yields the repeller automaton with the 5 loops

$$\{\overline{1}\}, \{\overline{01}\}, \{\overline{20}\}, \{\overline{201}\}, \{\overline{200}\} \quad (2.10)$$

and the 2 two combinations of loops without a common node

$$\{\overline{20}, \overline{1}\}, \{\overline{002}, \overline{1}\} \quad (2.11)$$

The topological polynomial is then

$$p(z) = 1 - z - 2z^2 - z^3 + z^4 \quad (2.12)$$

with the smallest root and the topological entropy

$$z = 0.480534, \quad h = \ln 2.08102 = 0.732857 \quad (2.13)$$

slightly larger than for the complete unimodal map.

2.2 Trimodal maps

In the generalization from bimodal to trimodal maps some new phenomena appear. Trimodal maps have bifurcations of co-dimension three and we have to describe a rather complicated bifurcation structure in 3 dimensional parameter space.

The first important observation is that a map like (2.2) *does not* have three critical points for all parameter values (a, b, c) . A minimum and a maximum point may merge, reducing the map to the unimodal case with a one-parameter bifurcation structure. Also the number of symbols changes from four symbols when the map is trimodal to two symbols when it is unimodal. This merging of critical points could be avoided by a restriction on the parameters, but that would exclude us from understanding the bifurcations that take place in maps of the Hénon type and therefore is it necessary to handle this problem.

The parameter space (a, b, c) looks rather complicated; figures 2.14, 2.18 and 2.22 are scans of the (a, b) plane at different constant c values, showing the parameter regions where a fixed point or a periodic orbit is stable. A simpler description of the bifurcation structures can be obtained by using the kneading value topological parameter space $(\kappa_1, \kappa_2, \kappa_3)$. The bifurcation parameter values for the fixed points and period 2 orbits are drawn as planes in this space in figure 2.17. The map is trimodal if $\kappa_1 > \kappa_2$ and $\kappa_3 > \kappa_2$. The border planes $\kappa_1 = \kappa_2$ and $\kappa_3 = \kappa_2$ are drawn in the figure; the trimodal bifurcations take place inside the skew-pyramidal region in this space. When the parameters of the function (a, b, c) change in such a way that we cross one border plane, we move into a one-dimensional unimodal parameter space and may reenter the three-dimensional parameter space again at a different point on a border plane. When we enter the unimodal region we can go through bifurcation of the MSS type and reenter at any point on the border planes of the trimodal map. The unimodal map will not have a negative Schwarzian close to the trimodal case so the stability of orbits may be different than for the logistic map.

The planes giving the bifurcations of orbits are obtained by determining the values $\tau_i^{\max}(S)$, $i \in \{1, 2, 3\}$, for a given orbit and drawing the planes $\kappa_i = \tau_i^{\max}(S)$. Table 2.1 gives the numerical values of τ_i^{\max} for the orbits of length 1, 2 and 3. Note

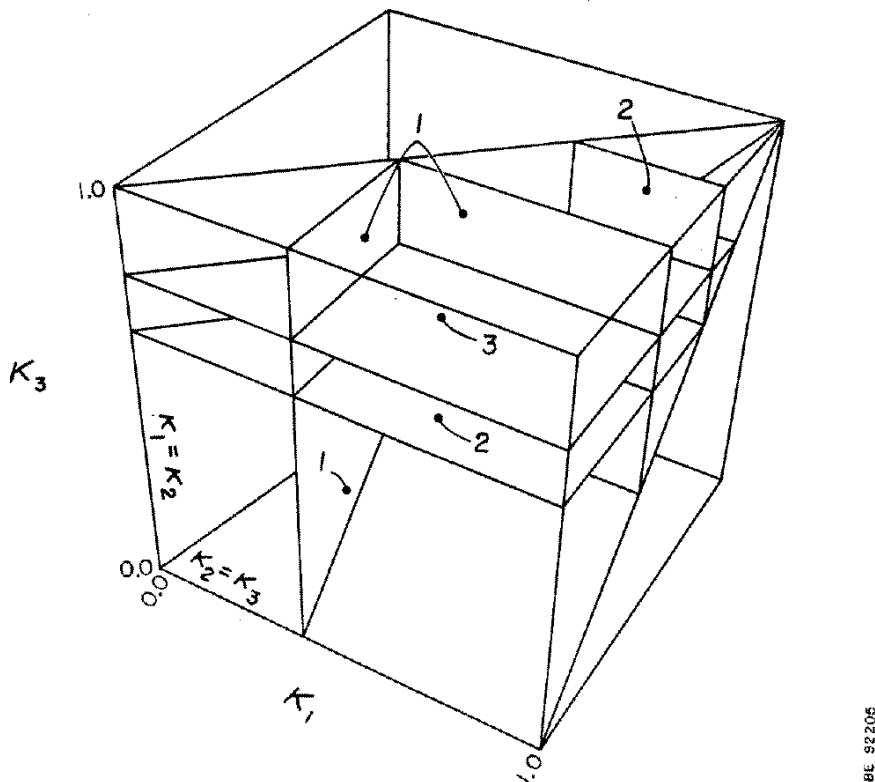


Figure 2.13: The bifurcation planes of fixed points in the trimodal map in the topological parameter space $(\kappa_1, \kappa_2, \kappa_3)$. The κ_2 axis is hidden behind the bifurcation planes.

that not all the orbits has all the three τ_i^{\max} -values. The conditions for an orbit to be admissible in the trimodal map follows from (2.6):

$$\begin{aligned}
 \tau_1^{\max}(S) &\leq \kappa_1 \\
 \tau_2^{\min}(S) &\geq \kappa_2 \\
 \tau_3^{\max}(S) &\leq \kappa_3.
 \end{aligned}
 \tag{2.14}$$

If these 3 conditions yield a box in the region within the border planes $\kappa_1 = \kappa_2$ and $\kappa_3 = \kappa_2$, the orbit always disappears in a bifurcation before the map gets unimodal, and the orbit can never change symbols without going through a super-stable value. If the box is only partly confined within the border planes, then the orbit exists and may be unstable also when the map is unimodal, and may change symbolic description without ever getting stable. The sign of the eigenvalue cannot change as long as the orbit remains unstable, so the sum of symbols which are either 1 or 3 has to remain odd or even.

S	τ_1^{\max}	S	τ_2^{\min}	S	τ_3^{\max}
				$\bar{3}$	$\bar{.30}$
		$\bar{2}$	$\bar{.2}$	$\bar{2}$	$\bar{.2}$
$\bar{1}$	$\bar{.12}$	$\bar{1}$	$\bar{.12}$		
$\bar{0}$	$\bar{.0}$				

$\bar{30}$	$\bar{.3300}$			$\bar{03}$	$\bar{.0330}$
$\bar{31}$	$\bar{.32}$	$\bar{31}$	$\bar{.32}$	$\bar{13}$	$\bar{.10}$
		$\bar{32}$	$\bar{.3102}$	$\bar{32}$	$\bar{.3102}$
$\bar{21}$	$\bar{.2112}$	$\bar{12}$	$\bar{.1122}$	$\bar{12}$	$\bar{.1122}$
$\bar{20}$	$\bar{.20}$	$\bar{02}$	$\bar{.02}$	$\bar{02}$	$\bar{.02}$
$\bar{10}$	$\bar{.1320}$	$\bar{01}$	$\bar{.0132}$		

S	τ_1^{\max}	S	τ_2^{\min}	S	τ_3^{\max}
$\bar{300}$	$\bar{.333000}$			$\bar{003}$	$\bar{.003330}$
$\bar{301}$	$\bar{.332}$	$\bar{301}$	$\bar{.332}$	$\bar{013}$	$\bar{.010}$
$\bar{230}$	$\bar{.233100}$	$\bar{302}$	$\bar{.331002}$	$\bar{302}$	$\bar{.331002}$
$\bar{330}$	$\bar{.300}$			$\bar{303}$	$\bar{.330}$
$\bar{331}$	$\bar{.301032}$	$\bar{331}$	$\bar{.301032}$	$\bar{313}$	$\bar{.323010}$
$\bar{231}$	$\bar{.232}$	$\bar{231}$	$\bar{.232}$	$\bar{312}$	$\bar{.322}$
$\bar{311}$	$\bar{.321012}$	$\bar{131}$	$\bar{.101232}$	$\bar{113}$	$\bar{.123210}$
$\bar{310}$	$\bar{.320}$	$\bar{031}$	$\bar{.032}$	$\bar{103}$	$\bar{.130}$
$\bar{320}$	$\bar{.313020}$	$\bar{032}$	$\bar{.031302}$	$\bar{203}$	$\bar{.2031130}$
$\bar{321}$	$\bar{.312}$	$\bar{132}$	$\bar{.102}$	$\bar{213}$	$\bar{.210}$
		$\bar{232}$	$\bar{.231102}$	$\bar{322}$	$\bar{.311022}$
		$\bar{332}$	$\bar{.302}$	$\bar{323}$	$\bar{.310}$
$\bar{221}$	$\bar{.221112}$	$\bar{122}$	$\bar{.111222}$	$\bar{212}$	$\bar{.211122}$
$\bar{220}$	$\bar{.220}$	$\bar{022}$	$\bar{.022}$	$\bar{202}$	$\bar{.202}$
$\bar{210}$	$\bar{.213120}$	$\bar{021}$	$\bar{.021312}$	$\bar{102}$	$\bar{.131202}$
$\bar{211}$	$\bar{.212}$	$\bar{121}$	$\bar{.112}$	$\bar{112}$	$\bar{.122}$
$\bar{201}$	$\bar{.201132}$	$\bar{012}$	$\bar{.011322}$	$\bar{012}$	$\bar{.011322}$
$\bar{200}$	$\bar{.200}$	$\bar{002}$	$\bar{.002}$	$\bar{002}$	$\bar{.002}$
$\bar{100}$	$\bar{.133200}$	$\bar{001}$	$\bar{.0011332}$		
$\bar{101}$	$\bar{.132}$	$\bar{011}$	$\bar{.012}$		

Table 2.1: The fixed points, period 2 and period 3 orbits in the trimodal map with the kneading values giving the topological bifurcation diagrams in figures 2.13, 2.17, 2.20 and 2.21.

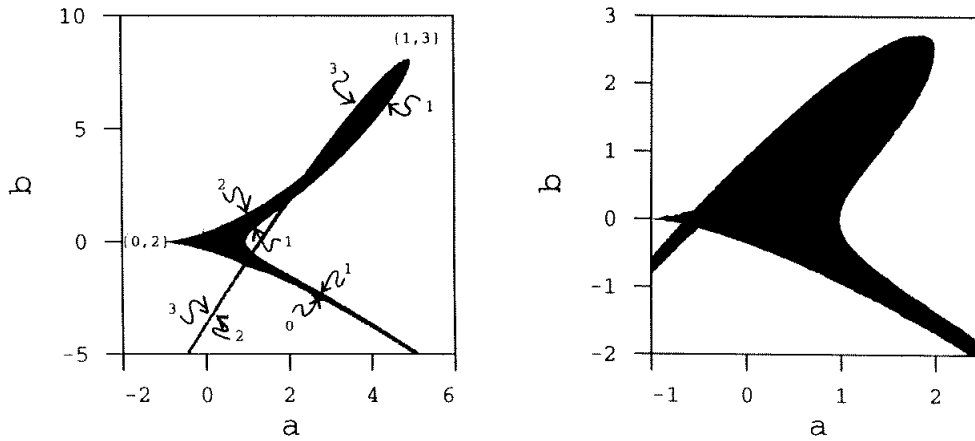


Figure 2.14: The area in parameter space (a, b) for the trimodal map where fixed points are stable, a) $c = 0.25$, b) $c = 0.5$.

2.2.1 Fixed points

In figure 2.13 the bifurcation diagram for the fixed points in $(\kappa_1, \kappa_2, \kappa_3)$ is drawn. The point $(1.0, 0.0, 1.0)$ corresponds to the complete trimodal repeller. This point is in figure 2.13 the corner closest to the viewer. Going downwards from this corner the figure can be read as follows; at the horizontal plane marked 3 the fixed point with symbolic description $\bar{3}$ becomes superstable and changes symbolic description to $\bar{2}$. When κ_3 decreases further, the two fixed points $\bar{2}$ disappear at the horizontal plane marked 2 in figure 2.13. The fixed point $\bar{1}$ disappears either at a plane with constant κ_1 or with constant κ_2 . If we let κ_1 decrease, the fixed point $\bar{1}$ changes symbolic description to $\bar{0}$ and the two fixed points $\bar{0}$ disappear at $\kappa_1 = 0$. Another possibility is that we let κ_2 increase and then the fixed point $\bar{1}$ changes symbolic description to $\bar{2}$ and the two fixed points $\bar{2}$ disappear at the vertical plane marked 2 in figure 2.13.

If we try to follow a fixed point $\bar{3}$ while κ_1 decreases or κ_2 increases we can pass into the unimodal map regime through the plane $\kappa_1 = \kappa_2$, without any bifurcations of the fixed point. In figure 2.13 we see that it is possible to enter the trimodal region at the plane $\kappa_2 = \kappa_3$ where the fixed point $\bar{1}$ exists but not the fixed point $\bar{3}$. We may therefore change the symbolic description of the fixed point by smooth parameter changes without ever making the fixed point stable. Since the sign of the derivative cannot change, the fixed point $\bar{3}$ can change only into $\bar{1}$, and the fixed point $\bar{2}$ only into $\bar{0}$.

We now compare figure 2.13 with two scans of the parameter plane (a, b) with $c = 0.25$ and $a = 0.5$, figure 2.14 a) and b). These scans should be thought of

as topological equivalent to surfaces cutting through the symbolic parameter space of figure 2.13. In figure 2.14 symbols 0 and 2 indicates planes at which a tangent bifurcation creates the fixed points $\bar{0}$ or $\bar{2}$. Symbols 1 and 3 indicate the planes where the fixed point $\bar{1}$ or $\bar{3}$ becomes unstable. The area indicated by $\{1, 3\}$ corresponds to parameter values for which the map is unimodal, and the fixed point with negative $f'(x)$ does not have a unique symbol but as one moves into the trimodal region the fixed point achieves either the symbolic description $\bar{1}$ or the symbolic description $\bar{3}$. For the area indicated by $\{0, 2\}$ the fixed point with positive $f'(x)$ does not have a unique symbol in the 4 letter alphabet, but may become either $\bar{0}$ or $\bar{2}$. Moving in these two areas corresponds to move around the corners of the boxes $\bar{1}$ or $\bar{2}$ in figure 2.13. To get around the corners one has to cross a unimodal region and consequently some symbols may change.

In the (a, b) plane all regions with a stable fixed point are connected; and this can be read out of the picture of the topological parameter space, figure 2.13. The two horizontal planes $\bar{3}$ and $\bar{2}$ are associated with one tail of a stable fixed point. As κ_2 increases in figure 2.13, this tail connects to the tail associated with the planes for $\bar{2}$ and $\bar{1}$ with constant κ_2 . Decreasing κ_1 in this tail gives the transition to the tail associated with the region between the constant κ_1 plane of $\bar{1}$ and the $\kappa_1 = 0$ line where $\bar{0}$ bifurcates. We see that this last region crosses the first region of the planes of $\bar{3}$ and $\bar{2}$, and this is also the case in the (a, b) plane in figure 2.14.

Figure 2.15 is a sketch of the (a, b) plane as in figure 2.14 but the sheets representing the different orbits are drawn in three dimensions to make the cusp bifurcations clearer. In this figure it is also clear that orbits may change symbols when moving around one of the cusp singularities.

In figure 2.16 the function $f(x)$ is drawn for a sequence of values for which the fixed point change symbol from $\bar{1}$ to $\bar{3}$.

2.2.2 Period 2 orbits

Figure 2.17 shows the planes in the topological parameter plane where both the fixed points and the period 2 orbits bifurcate. This figure is interpreted in a similar way as figure 2.13. We know from the bimodal map that period 2 orbits may exhibit a swallowtail crossing, and we do find swallowtails in figure 2.17. On the top plane, $\kappa_3 = 1$, we find the same swallowtail crossing as in the bimodal plane in figure 2.5. We adapt a convention to describe crossings such that $\overline{\{s_1, s_2\}, \{s_3, s_4\}}$ is equivalent with the four symbol strings $\overline{s_1 s_3}, \overline{s_1 s_4}, \overline{s_2 s_3}, \overline{s_2 s_4}$ and the notation $\overline{s_1 \{s_2, s_3, s_4\}}$ is short for the three orbits $\overline{s_1 s_2}, \overline{s_1 s_3}$ and $\overline{s_1 s_4}$. The symbols of the orbits in this crossing are $\overline{\{1, 2\}\{0, 1\}}$ (the orbits $\bar{10}, \bar{1}, \bar{20}, \bar{21}$) as in the bimodal case, and the

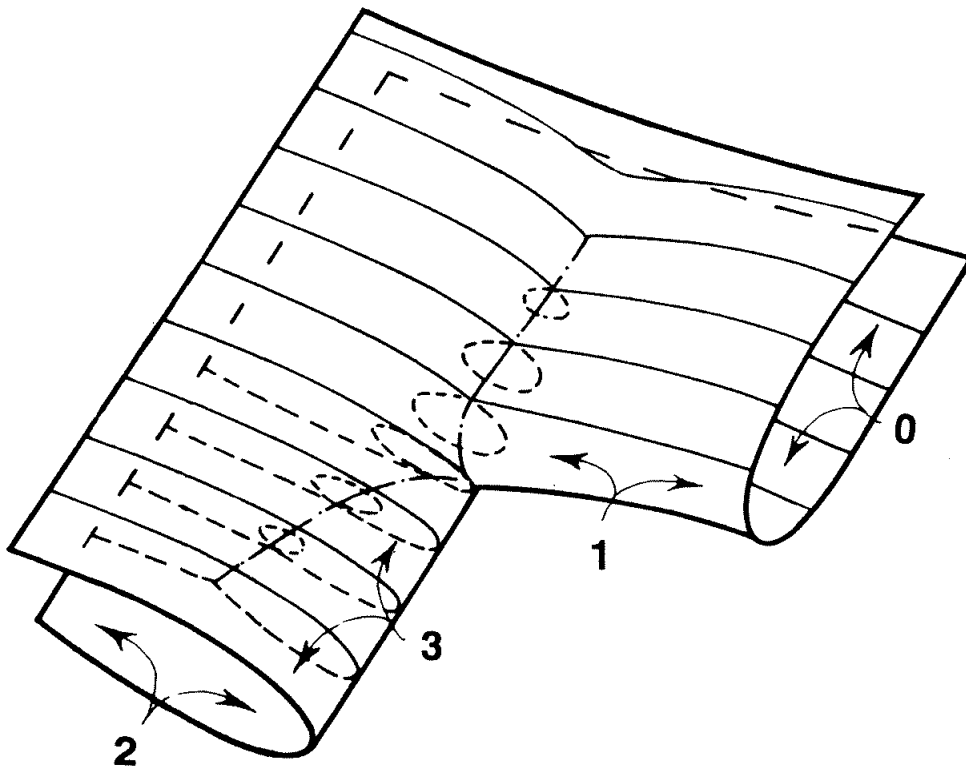


Figure 2.15: Coexistence of fixed points in the (a, b) plane with constant c for the trimodal map.

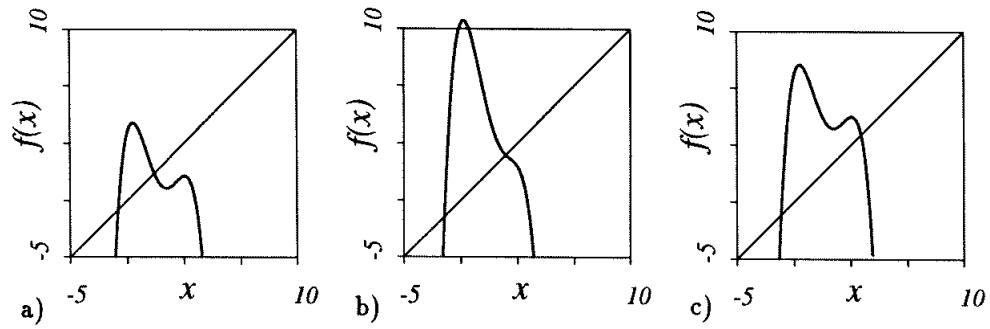


Figure 2.16: The function $f(x)$ for different parameter values in the region where a fixed point changes symbol from $\bar{1}$ to $\bar{3}$, $c = 0.25$, a) $a = 3, b = 2$ b) $a = 4.77, b = 7$ c) $a = 3, b = 6$.

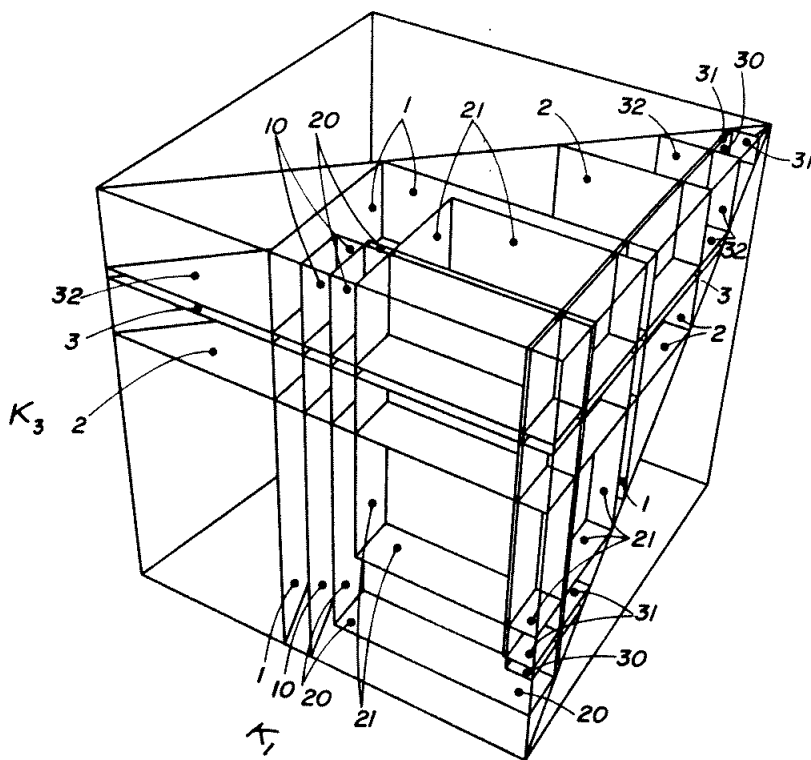


Figure 2.17: The bifurcation planes of period 2 orbits in the trimodal map in the topological parameter space $(\kappa_1, \kappa_2, \kappa_3)$.

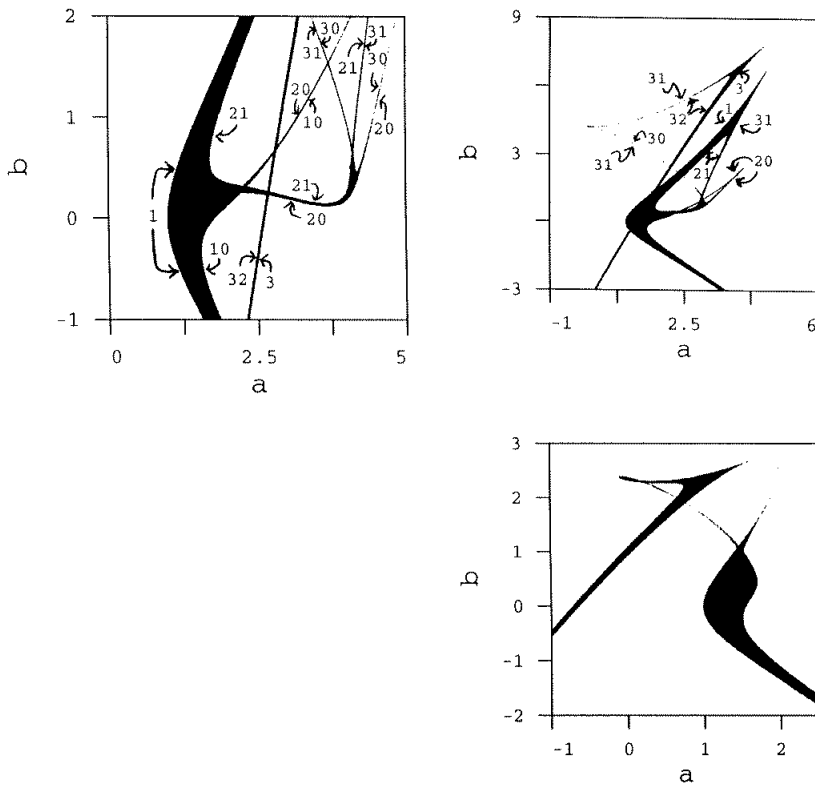


Figure 2.18: The area in parameter space (a, b) for the trimodal map where period 2 orbits are stable. a) $c = 0.2$, b) $c = 0.25$ c) $c = 0.5$.

structure is the same, only the scale is slightly changed since we here use base 3 to calculate κ_1 and κ_2 .

In figure 2.17 we find another swallowtail for $\kappa_2 = 0$ which includes the orbits $\overline{\{2, 3\}\{0, 1\}}$. The two swallowtail crosses are directly connected to each other by having the tail $\overline{2\{0, 1\}}$ in common. The scan of the parameter plane (a, b) with $c = 0.2$ in figure 2.18 a) shows these two swallowtail crosses and the common tail. In figure 2.18 the label 1 indicates the plane where the fixed point $\bar{1}$ goes through a period doubling. The labels 20 and 31 indicate the tangent bifurcations which create the two period 2 orbits, and labels 10, 21 and 30 indicate planes where the respective period 2 orbits become unstable.

Figure 2.18 b) shows that at slightly larger value of c the swallowtails crosses get closer together. The figure also shows other cusp points that can be found in the topological parameter space in figure 2.17, and we see how the different tails are connected. Notice also that in the region of figure 2.14 where the fixed point changes

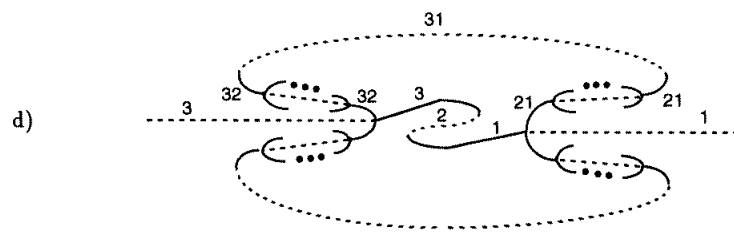
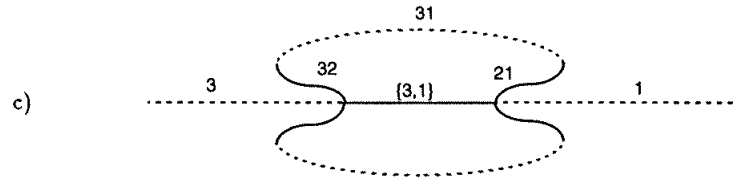
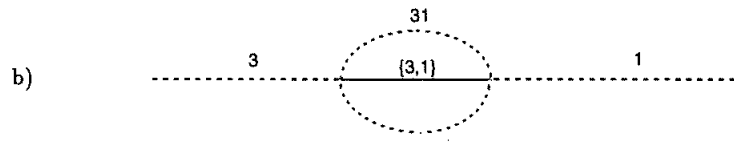
symbolic description from $\bar{1}$ to $\bar{3}$ there is no period 2 orbit that change symbol. When a fixed point becomes unstable close to an inflection point, the bifurcation can not be a period doubling bifurcation, but is an inverse bifurcation where the fixed point becomes unstable by removing an unstable period 2 orbit. In this case the removed orbit is $\bar{3}\bar{1}$. Figure 2.19 shows such bifurcations at different one-parameter scans of the parameter space. In figure 2.19 a) the fixed point changes symbol without going through any bifurcations. In figure 2.19 b) the fixed point becomes stable in a bifurcation which creates the unstable period 2 orbit $\bar{3}\bar{1}$ and the fixed point changes symbols when it is stable but not superstable. At a parameter scan closer to the $\{1, 3\}$ cusp in figure 2.14 a) we get figure 2.19 c) where the fixed point has a bifurcation with a stable period 2 orbit, which in turn was created in a tangent bifurcation together with the unstable period 2 orbit. Finally, in figure 2.19 d) below the $\{1, 3\}$ cusp all orbits change symbolic description only at superstable points. One may also find paths in parameter space where the bifurcations are not symmetric, one has a finite number of bifurcations, etc. The important structure of the cusp and the change of symbols are however described by these four figures.

The only period 2 orbit existing in figure 2.19 a) is the orbit $\bar{3}\bar{0}$. This orbit do not change symbol here but at one of the two cusp bifurcations; either to $\bar{1}\bar{0}$ at the cusp $\overline{\{1, 2, 3\}0}$ middle-right at figure 2.18 b), or to $\bar{3}\bar{2}$ at the cusp $\overline{3\{0, 1, 2\}}$ to the left in figure 2.18 b). Consequently a loop around the cusp the fixed point changes the description from $\bar{1}$ to $\bar{3}$ but there is no change of any period 2 orbit.

2.2.3 Period 3 orbits

Period 3 orbits form a rather complicated structure in the trimodal map parameter space, and without the topological parameter space bifurcation diagrams would it be difficult to have an overview of the bifurcations. In figure 2.20 all bifurcation planes corresponding to the values of τ_i^{\max} listed in table 2.1 are drawn. To simplify the reading, the diagram is also drawn in figure 2.20 with the labels restricted to the swallowtail crossings on the planes $\kappa_1 = 1$, $\kappa_2 = 0$ and $\kappa_3 = 1$.

A general observation is that there are many orbits restricted by bifurcation planes to the interior of the trimodal region. Out of 20 orbits there are 6 orbits that only have two τ_i values giving only two sides of the box, and there are 2 orbits which have three values of τ_i but with one corner outside the trimodal region. 4 orbits have the corner of the box in parameter space on the edge of the trimodal region. Hence in all 12 period 3 orbits cannot change the symbolic dynamics description without getting superstable. In contrast for the period 2 orbits only 2 out of 6 orbits cannot change symbols, and all the fixed points may change symbols.



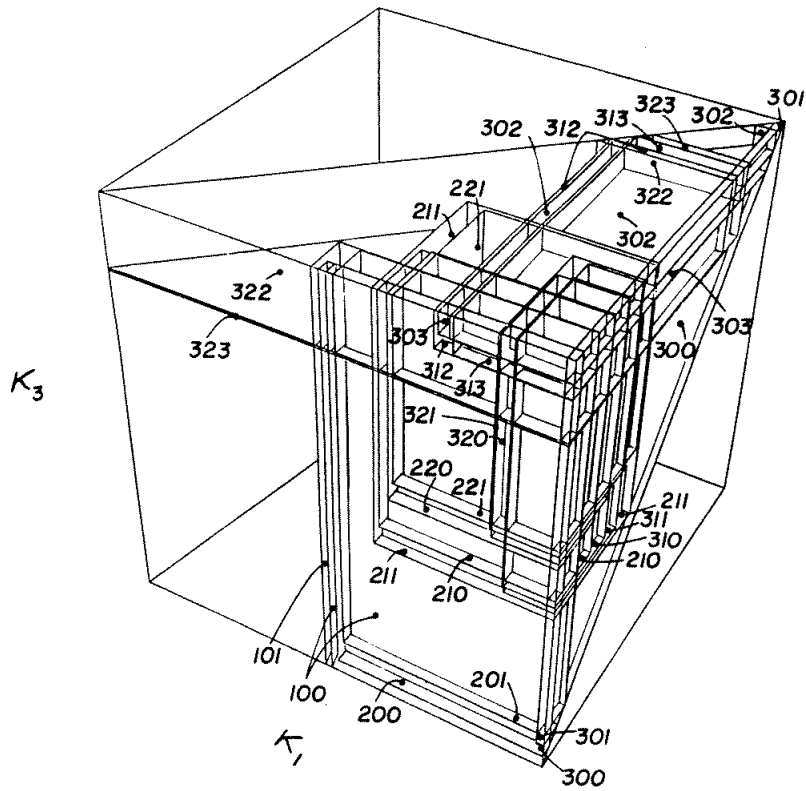


Figure 2.20: The bifurcation planes of period 3 orbits in the trimodal map in the topological parameter space $(\kappa_1, \kappa_2, \kappa_3)$, each plane labeled by the symbols for the period 3 orbit created at this parameter value.

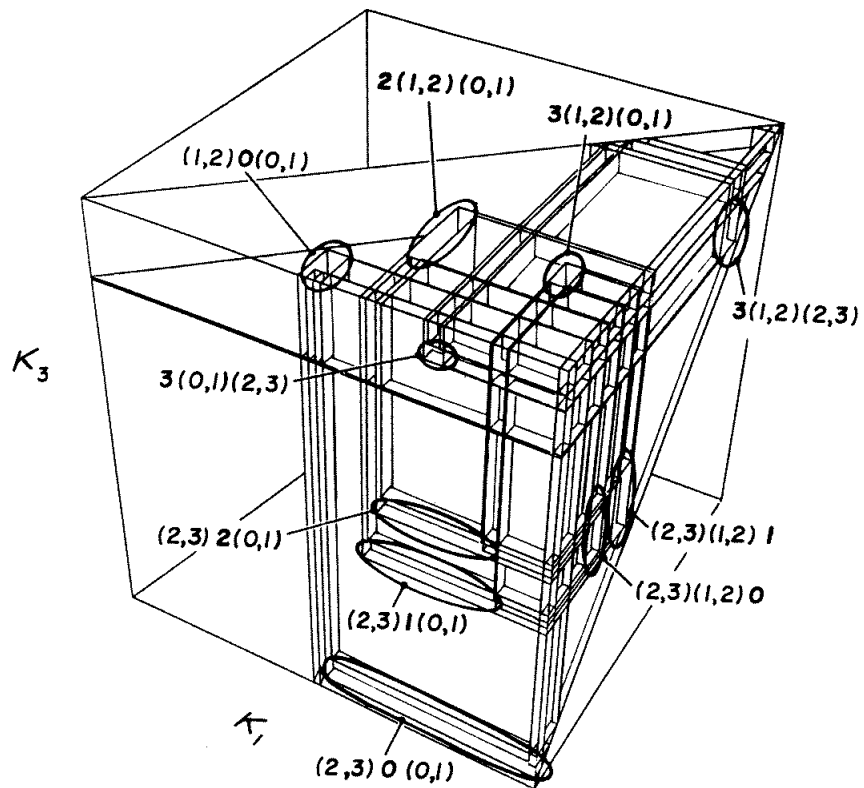


Figure 2.21: The same as figure 2.20, but labeled with the swallowtail crossings rather than the individual period 3 orbits.

For long orbits only a small fraction of the orbits can change symbols. For long symbol strings there are few orbits that do not have any symbols $(i - 1)$ or (i) such that τ_i does not exist, or that τ_2^{\min} is larger than either τ_1^{\max} or τ_3^{\max} . This is good news because there is relatively few long orbits that we have to worry about whether we use the right symbolic description or not, but some very long orbits will also have the possibility of changing symbolic dynamics without becoming stable.

The plots in figure 2.22 show some scans of the parameter plane (a, b) where the period 3 orbits are stable. The swallowtail crosses are labeled as (and should be compared to) the topological swallowtail crosses in figure 2.21. In figure 2.21 there is a structure consisting of the six crosses $\overline{2\{1, 2\}\{0, 1\}}$, $\overline{3\{1, 2\}\{0, 1\}}$, $\overline{\{2, 3\}2\{0, 1\}}$, $\overline{\{2, 3\}1\{0, 1\}}$, $\overline{\{2, 3\}\{1, 2\}0}$ and $\overline{\{2, 3\}\{1, 2\}1}$ that are connected by tails to each other but not to any other crosses, and they all bifurcate inside the bifurcation box of $\overline{112}$, inside the trimodal region. All these orbits disappear before the map becomes unimodal and they do not change any symbols by moving around a cusp structure without getting superstable. Figures 2.22 a)–f) show that increasing the parameter c makes the (a, b) plane to a surface deeper and deeper in the topological parameter space. In figure 2.22 f) the surface cuts below the box $\overline{112}$, and no structure from the six crosses remains. Each of the boxes in the structure is connected to a swallowtail cross in the three corners of the box. If a box moves above the (a, b) surface, these three crosses have to merge to one cross. If the pruning box of the orbit $\overline{320}$ in figure 2.21 moves above the (a, b) parameter plane, then the three crosses $\overline{3\{1, 2\}\{0, 1\}}$, $\overline{\{2, 3\}2\{0, 1\}}$ and $\overline{\{2, 3\}\{1, 2\}0}$ which have $\overline{320}$ as the only common orbit must merge together. This is exactly the bifurcation taking place in figure 2.22 as the value of c increases. There are other possible ways for the crossings to merge, but a 2-dimensional parameter plane cannot have other mergings of the bifurcation structure than those that can be obtained by moving a surface in the $(\kappa_1, \kappa_2, \kappa_3)$ space.

2.3 Higher n -modal maps

For four-modal and higher n -modal maps it is difficult to draw the n -dimensional topological parameter space bifurcation diagrams, but we can still use symbols to understand possible bifurcation structures.

A swallowtail crossing for a period m orbit in a n -modal map has the form

$$\overline{\{s_1, s'_1\}s_2 \cdots s_{j-1}\{s_j, s'_j\}s_{j+1} \cdots s_m} \quad (2.15)$$

where $s_i, s'_i \in \{0, 1, \dots, n\}$ and $|s_i - s'_i| = 1$ (neighbor symbols). A tail from this

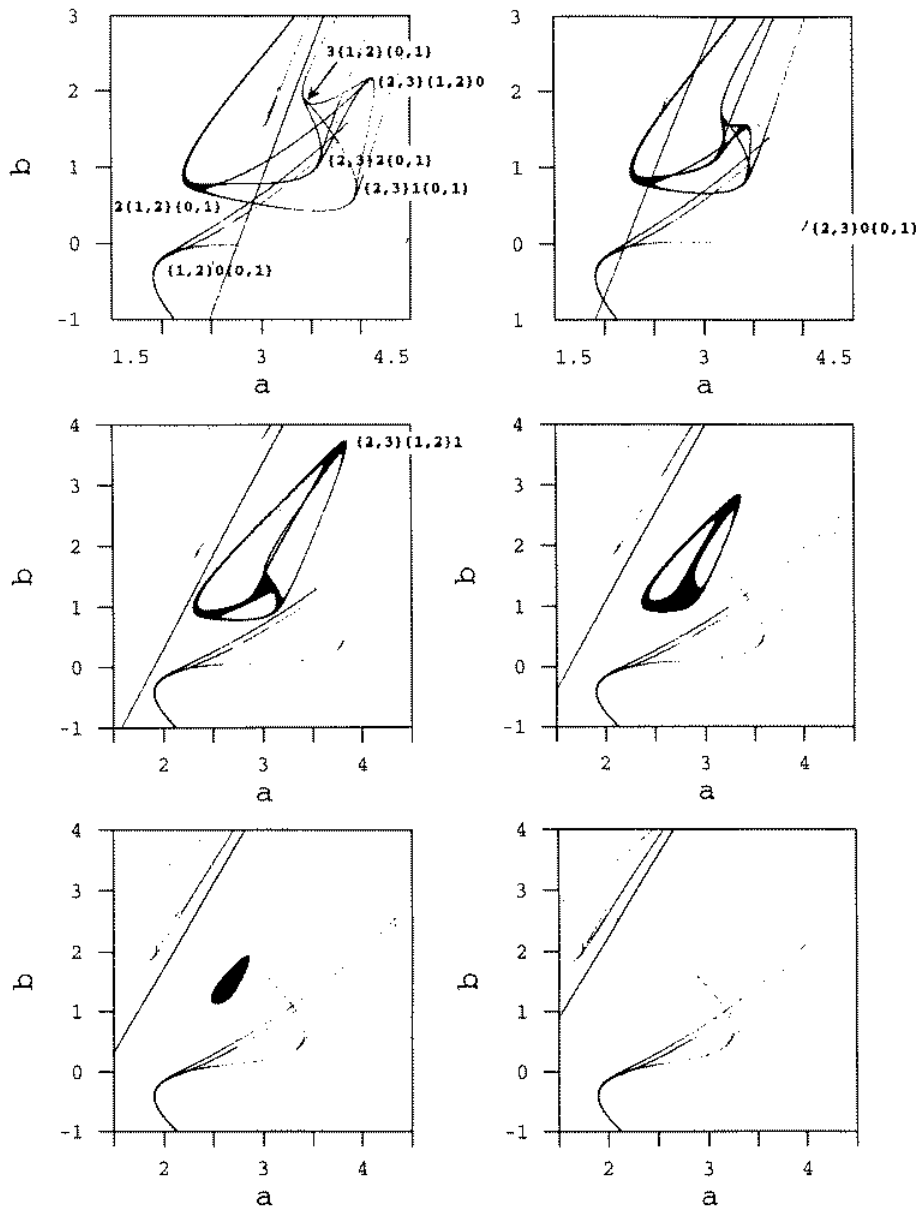


Figure 2.22: The area in parameter space (a, b) for the trimodal map where period 3 orbits are stable. a) $c = 0.195$, b) $c = 0.21$ c) $c = 0.22$ d) $c = 0.23$ e) $c = 0.24$ f) $c = 0.25$.

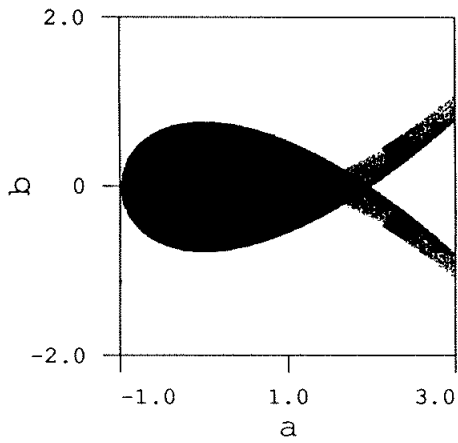


Figure 2.23: The area in parameter plane of map (2.18) with stable fixed point.

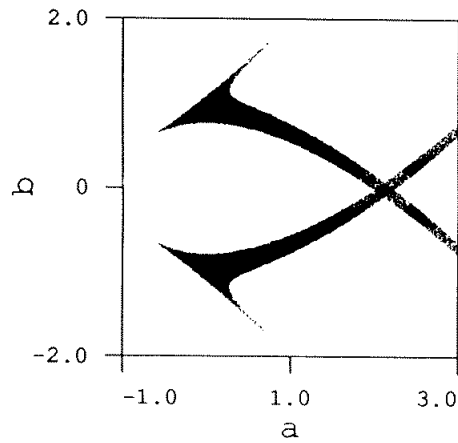


Figure 2.24: The area in parameter plane of map (2.18) with stable period 2 orbits.

crossing is

$$\overline{\{s_1, s'_1\} s_2 \cdots s_{j-1} s_j s_{j+1} \cdots s_m} \quad (2.16)$$

and this tail connects the crossing to another swallowtail crossing

$$\overline{\{s_1, s'_1\} s_2 \cdots s_{k-1} \{s_k, s'_k\} s_{k+1} \cdots s_m} \quad (2.17)$$

where $k \neq j$ if both crossings exist. By using such rules it is easy to find all connected swallow tails, and the possible merging and disappearances of the crossings.

2.4 The $- + -$ bimodal map

To complete the discussion of bimodal maps we can also find the bifurcation diagrams for the bimodal map with $f'(x) < 0$ for $x < x_{c1}$ and $x > x_{c2}$ and with $f'(x) > 0$ for $x_{c1} < x < x_{c2}$, denoted $- + -$. We denote the bimodal map (2.1) according to the sign of $f'(x)$: $+ - +$. We will here just present the bifurcation diagrams and the numerical results from the map

$$f(x) = -x^3 + ax - b \quad (2.18)$$

as the results are very similar to the $+ - +$ bimodal map. The kneading values κ_1 and κ_2 yield a symbolic parameter plane, and bifurcations lines for periodic orbits of length 1, 2, 3 and 4 are drawn in figures 2.25, 2.27 and 2.29. The parameter regions (a, b) with stable periodic orbits for the map (2.18) are drawn in figures 2.23, 2.24, 2.26 and 2.28. The line $\kappa_2 = 1 - \kappa_1$ corresponds to the line $b = 0$ in map (2.18)

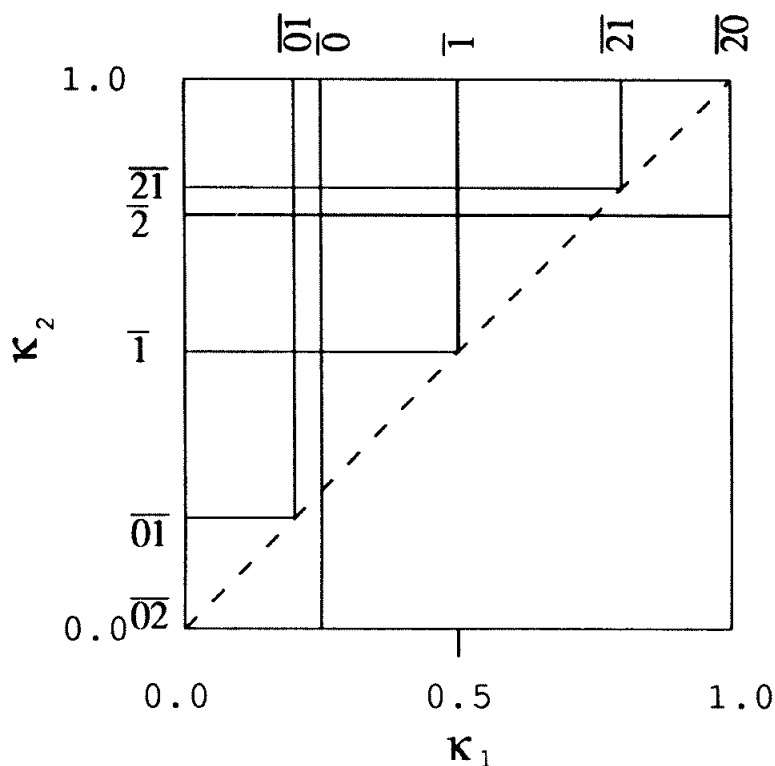


Figure 2.25: The bifurcation lines of the fixed points and period 2 orbit in the symbolic parameter plane of the $- + -$ bimodal map

and at the point $\kappa_1 = 0, \kappa_2 = 1$ is the point corresponding to the complete binary repeller. The line $\kappa_2 = \kappa_1$ is the bifurcation line where the two extremum points merge together.

The period 3 and period 4 bifurcation diagrams are different but of the same structure as for the $+ - +$ bimodal map. The period 3 orbits yield two swallowtails and the period 4 orbits yield five swallowtails.

The bifurcations of the fixed points and the period 2 orbits yield a slightly different bifurcation structure than for the $+ - +$ bimodal map. In the $+ - +$ map the stable fixed point $\bar{1}$ and all the period 2 orbits existed only in the bimodal regime; $\kappa_2 < \kappa_1$. For the $- + -$ map the two stable fixed points $\bar{0}$ and $\bar{2}$ and the period two orbit $\bar{20}$ exist also outside the bimodal regime $\kappa_2 > \kappa_1$. This gives a different cusp structures similar to those examined in the trimodal map.

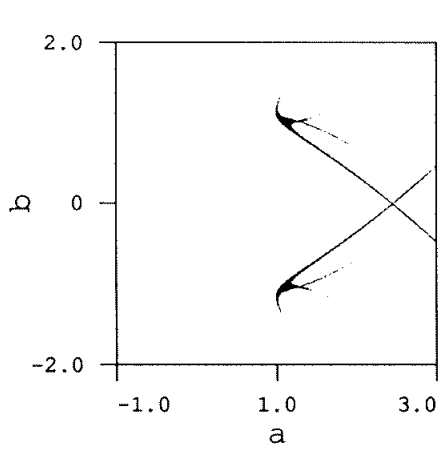


Figure 2.26: The area in parameter plane of map (2.18) with stable period 3 orbits

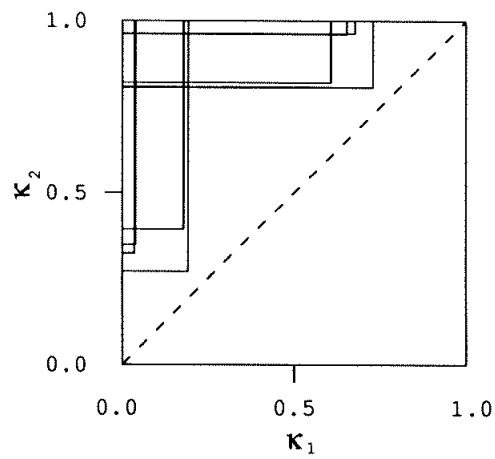


Figure 2.27: Bifurcation lines of the period 3 orbit in the $- + -$ bimodal map

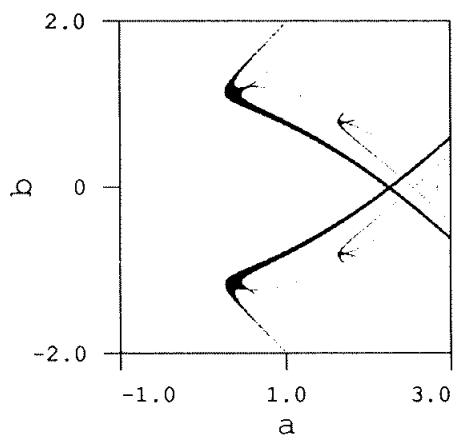


Figure 2.28: The area in parameter plane of map (2.18) with stable period 4 orbits

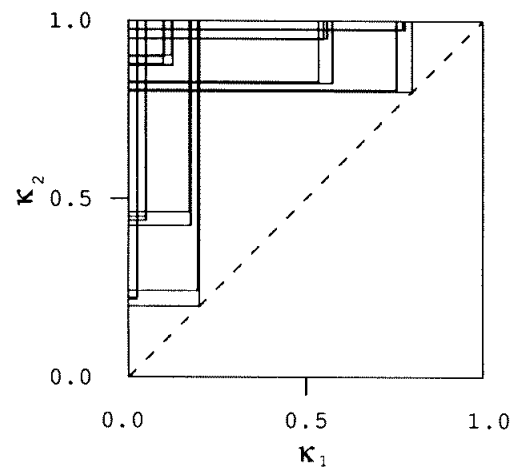


Figure 2.29: Bifurcation lines of the period 4 orbit in the $- + -$ bimodal map

